

Novel benzofuran inhibitors of human mitogen-activated protein kinase phosphatase-1

John S. Lazo,^{a,b,*} Ruth Nunes,^{c,d} John J. Skoko,^{a,b} Pierre E. Queiroz de Oliveira,^{a,b}
Andreas Vogt^{a,b} and Peter Wipf^{a,c,d}

^aThe University of Pittsburgh Drug Discovery Institute, University of Pittsburgh, Pittsburgh, PA 15261, USA

^bDepartment of Pharmacology, University of Pittsburgh, Pittsburgh, PA, 15261, USA

^cDepartment of Chemistry, University of Pittsburgh, Pittsburgh, PA 15261, USA

^dCombinatorial Chemistry Center, University of Pittsburgh, Pittsburgh, PA 15261, USA

Received 25 February 2006; revised 12 April 2006; accepted 13 April 2006

Available online 15 May 2006

Abstract—Protein tyrosine phosphatases have a central role in the maintenance of normal cellular functionality. For example, PTP1B has been implicated in insulin-resistance, obesity, and neoplasia. Mitogen-activated protein kinase phosphatase-1 (MKP-1 or DUSP1) dephosphorylates and inactivates mitogen-activated protein kinase (MAPK) substrates, such as p38, JNK, and Erk, and has been implicated in neoplasia. The lack of readily available selective small molecule inhibitors of MKP family members has severely limited interrogation of their biological role. Inspired by a previously identified inhibitor (NSC 357756) of MKP-3, we synthesized seven NSC 357756 congeners, which were evaluated for in vitro inhibition against several protein phosphatases. Remarkably, none displayed potent inhibition against MKP-3, including the desamino NSC 357756 analog NU-154. Interestingly, NU-154 inhibited human PTP1B in vitro with an IC₅₀ value of 24 ± 1 μ M and showed little inhibition against Cdc25B, MKP-1, and VHR phosphatases. NU-126 [2-((*E*)-2-(5-cyanobenzofuran-2-yl)vinyl)-1*H*-indole-6-carbonitrile] inhibited MKP-1 and VHR in vitro but was less active against human MKP-3, Cdc25B, and PTP1B. The inhibition of MKP-1 by NU-126 was independent of redox processes. The benzofuran substructure represents a new potential scaffold for further analog development and provides encouragement that more selective and potent inhibitors of MKP family members may be achievable.

© 2006 Elsevier Ltd. All rights reserved.

1. Introduction

Protein tyrosine phosphorylation is a prominent mechanism by which mammalian cells alter protein functionality.^{1,2} The phosphorylation status of a given protein is dynamically controlled by kinases and phosphatases and is generally highly regulated. The 107 protein tyrosine phosphatases (PTPs) found in the human genome are defined by the active site sequence C(X)₅R, with X being any amino acid, and they are critical regulators

of mammalian cell proliferation, differentiation, and apoptosis. PTPs can be divided into at least four subfamilies based on their tertiary structure: classical phosphotyrosine specific PTPs, dual specificity phosphatases, Cdc25 phosphatases, and low molecular weight PTPs.³ The classical PTP, PTP1B, is among the best studied human PTPs in part because it has been critically implicated in the pathobiology of diabetes and obesity.⁴ Moreover, PTP1B is an important determinant of the latency and type of tumors in a p53-tumor suppressor deficient background through its role in the regulation of B-cell development.⁵ A considerable number of potent and selective small molecule inhibitors of PTP1B have been identified.^{3,6} In contrast, there is a dearth of potent and selective pharmacological inhibitors for members of the other PTP subfamilies. For example, there are no potent inhibitors of MKP-1, which dephosphorylates p38, JNK, and Erk1/2.^{7–9} This is unfortunate because MKP-1 has been associated with human neoplasia and is an attractive potential therapeutic target. MKP-1 is highly expressed in prostate, breast, gastric,

Abbreviations: DTT, dithiothreitol; IC₅₀, concentration of compound required for 50% inhibition; Erk, extracellular signaling-related protein kinase; MAPK, mitogen-activated protein kinase; MKP-1, mitogen-activated protein kinase phosphatase-1; OMFP, 3-*O*-methylfluorescein phosphate; PBS, phosphate-buffered saline; PTP, protein tyrosine phosphatase; ROS, reactive oxygen species.

Keywords: Protein tyrosine phosphatases; Enzyme inhibition; Cancer; Mitogenic signaling; Structure–activity relationship.

* Corresponding author. Tel.: +1 412 648 9200; fax: +1 412 648 9009; e-mail: lazo@pitt.edu

and renal cancer.^{10–12} In patients with ovarian cancer, MKP-1 expression is correlated with decreased progression-free survival.¹³ Liao et al.¹¹ reported that reduction of MKP-1 in human pancreatic cells ablated soft agar colony formation and tumorigenicity. Others have found MKP-1 protects cells from apoptosis induced by cisplatin, UV irradiation, and proteasome inhibitors.^{14–16}

It has been hypothesized that selective inhibitors of PTP should be achievable because of the differences in the active site surface features of at least some of the family members.² Lund et al.⁶ illustrated how low affinity ligands can be used with structural information to create potent inhibitors that were more selective for PTP β than other classical PTPs. Regrettably, structural information about MKP-1 is lacking. Recently, we identified the first cell-active small molecule inhibitor of MKP-1, the alkaloid sanguinarine, using a high content cellular chemical complementation assay.¹⁷ Sanguinarine, however, has a number of other reported effects including inhibition of protein kinase A, suppression of growth factor mediated angiogenesis, reduction of adhesion molecule expression, and inhibition of nuclear factor-

κ B-mediated transcription.¹⁸ Thus, more selective small molecule inhibitors are clearly desirable.

As a starting point, we used a small molecule inhibitor of MKP-3, namely NSC 357756 (6-(4,5-dihydro-1*H*-imidazol-2-yl)-2-(2-[5-(4,5-dihydro-1*H*-imidazol-2-yl)-benzofuran-2-yl]-vinyl)-1*H*-indol-3-ylamine) (Fig. 1), which we previously identified with a high content cell-based assay.¹⁹ This is justified because human MKP-3 shares 36% amino acid identity with human MKP-1 but the 11 amino acid catalytic domain is 82% identical (Table 2). NSC 357756 has also been reported to inhibit a Zn-dependent metalloprotease, namely anthrax lethal factor protease, which decreases the phosphorylation and activation of Erk.²⁰ Regrettably, we have been unable to obtain or synthesize additional quantities of this compound for further analysis. In fact, spectroscopic information on NSC 357756 is not available, and therefore we have been unable to independently confirm its structure. We now report on the use of the known desamino congener of NSC 357756 as well as the successful synthesis of analogs. Surprisingly, we found that some of these analogs are selective in vitro inhibitors of MKP-1 or PTP1B.

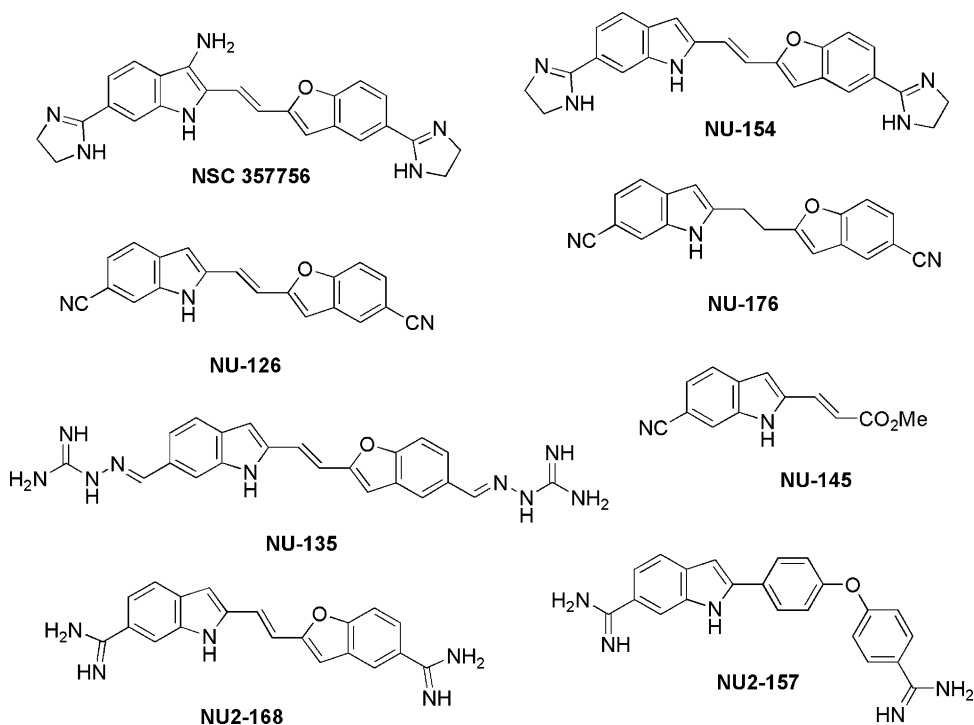


Figure 1. The chemical structures of NSC 357756 and newly synthesized analogs.

Table 1. Mean in vitro IC₅₀ values (μ M \pm SEM, $n = 4$) against human recombinant protein phosphatases

	NU-126	NU-135	NU-154	NU-176	NU-145	NU2-168	NU2-157
MKP-1	28.8 \pm 2.9	57.9 \pm 4.1	>100	47.6 \pm 3.8	>100	>100	>100
MKP-3	>400	73.2 \pm 6.3	>100	>100	ND ^a	73.3 \pm 4.0	70.0 \pm 4.2
Cdc25B	>400	>100	>100	>100	ND	ND	ND
PTP1B	>100	81.6 \pm 0.4	23.6 \pm 0.3	>100	ND	ND	ND
VHR	38.1 \pm 2.8	>100	>100	47.4 \pm 3.9	ND	ND	ND

^a Not determined.

2. Results

Although previously published results with an NSC 357756 sample provided by the U.S. National Cancer Institute suggested it was an inhibitor of MKP-3, we have concluded after repeated unsuccessful attempts that NSC 357756 was not a synthetically tractable compound. Consequently, we constructed five simplified indole analogs, which retained the fundamental benzofuran pharmacophore (Fig. 1). We also synthesized NU-145, which is a substructure of NU-126 and NU-176, and NU2-157, which lacked the benzofuran moiety. Surprisingly, we found no potent in vitro inhibitors of MKP-3, although NU2-168 and NU2-157 inhibited MKP-3 with IC_{50} values of 73.3 and 70.0 μ M, respectively (Table 1). The bis-nitrile NU-126, however, inhibited the dual specificity phosphatases MKP-1 and VHR with IC_{50} values of 28.8 ± 2.9 μ M and 38.1 ± 2.8 μ M (Fig. 2 and Table 1); at 100 μ M NU-126 inhibited PTP1B by only 30% and at 400 μ M it inhibited Cdc25B and MKP-3 by 30–40%. The reduced NU-176 with the flexible ethane linker connecting the two heterocyclic cores also retained inhibitory activity against MKP-1 and VHR, while against MKP-3, Cdc25B, and PTP1B it caused only 12%, 2%, and 33% inhibition, respectively. The bisaminoguanidine NU-135 exhibited IC_{50} values of 50–100 μ M against MKP-1, MKP-3, and PTP1B and at 100 μ M caused 28% and 46% inhibition of Cdc25B and VHR, respectively. NU2-168 and NU2-157 lack any significant activity against MKP-1. Interestingly, the bisimidazoline NU-154 inhibited PTP1B with an IC_{50} of 23.6 ± 0.3 μ M and had little activity against the other four phosphatases at 100 μ M.

Because of the selectivity profile and relative potency of NU-126, we examined this compound in greater detail. NU-126 also inhibited the dephosphorylation of the phosphorylated Erk duodecapeptide MAP (177–189) by MKP-1 with an IC_{50} of ~ 50 μ M (Fig. 3A). The dephosphorylation of this peptide by VHR was also inhibited by NU-126, although we only examined concentrations of 25 μ M and lower. Using the entire Erk protein as a substrate revealed a concentration-dependent inhibition by NU-126 with an IC_{50} of ~ 20 μ M (Fig. 4B).

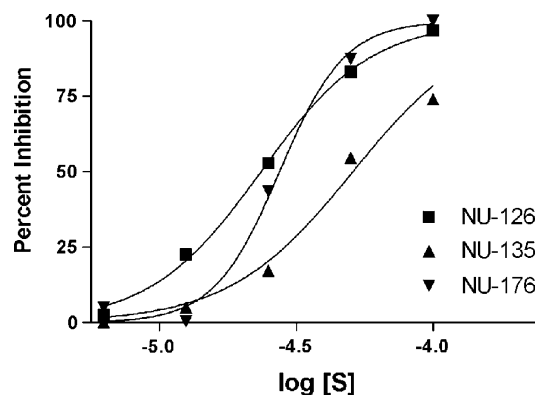


Figure 2. Concentration-dependent inhibition of MKP-1. Recombinant human MKP-1 was incubated with various concentrations of NU-126 (square), NU-135 (triangle), or NU-176 (inverted triangle) and enzyme activity determined as described in Section 4.

Some protein tyrosine phosphatases appear to be sensitive to intracellular oxidants, such as H_2O_2 or some *para*-quinones, due to the low pK_a of the catalytic cysteine.²¹ Thus, we examined the reversibility of NU-126 inhibition in vitro using a previously described dilution assay.²¹ As illustrated in Figure 5A, pre-incubation of MKP-1 for 20 min or less in the absence of the substrate did not alter the inhibitory actions of NU-126 reflective of a reversible inhibitor. In addition, incubation with concentrations of the reductant DTT of 10 or 25 mM did not alter the IC_{50} values nor did co-incubation with catalase (Fig. 5B). Thus, it appears NU-126 functions as a reversible inhibitor and did not rely on the oxidation of the catalytic cysteine to inactivate MKP-1. A kinetic analysis of MKP-1 inhibition with OMFP as a substrate supported a mixed rather than a true competitive model (Fig. 6).

3. Discussion

The protein tyrosine phosphatases have a critical role in regulating mammalian cell biology¹ and, consequently, there is considerable interest in identifying small molecule regulators of protein tyrosine family members, including the dual specificity phosphatase subfamily.

Table 2. Consensus sequence and predicted hydrophobicity for the catalytic sites in protein tyrosine phosphatases

Protein	Amino acid sequence							Mean hydrophobicity	Mean α moment	Mean β moment
MKP-1	F	V	H	C ²⁵⁸	Q	A	G I S R S	0.08	0.36	0.07
MKP-3	L	V	H	C ²⁹³	L	A	G I S R S	0.24	0.49	0.09
CDC25B	I	F	H	C ⁴⁸⁷	E	F	S S E R G	-0.02	0.24	0.01
PTP1B	V	V	H	C ²¹⁵	S	A	G I G R S	0.19	0.41	0.04
VHR	L	V	H	C ¹²⁴	R	E	G Y S R S	-0.31	0.27	0.01
Consensus	X	V/F	H	C	X	X	G/S X X R X			

Color coding of the amino acids was generated using the default settings of EMBL-EBI Protein Colourer in which the more hydrophobic amino acids are red, charged are green, sulfur-containing are yellow, and neutral amino acids are blue.

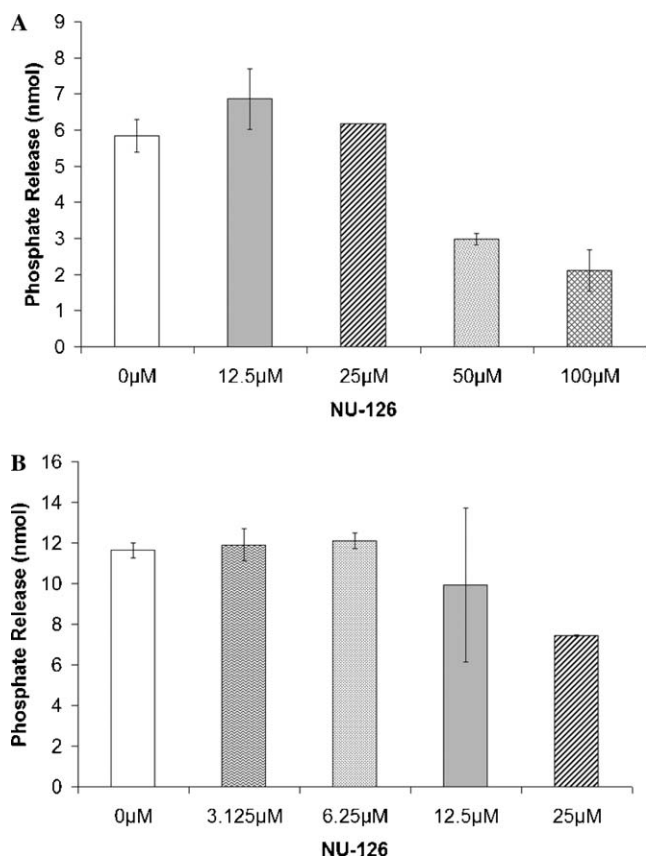


Figure 3. Inhibition of MKP-1- and VHR-mediated dephosphorylation of Erk phosphopeptide by NU-126. Human recombinant MKP-1 (66 μM) (A) or VHR (107 μM) (B) was incubated with 107 μM MAP (177–189) phosphopeptide in the presence or absence of various concentrations of NU-126 for 1 h. The release of free phosphate was determined using a malakite green assay.

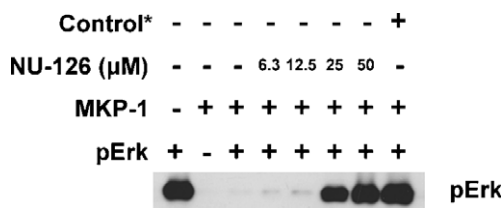


Figure 4. Inhibition of Erk dephosphorylation by NU-126. Phosphorylated Erk (0.67 $\mu\text{g}/\text{ml}$) was incubated with recombinant human MKP-1 in the presence of 0–50 μM NU-126 or 50 μM sanguinarine. Control* was DMSO vehicle alone. After incubation at 37 $^{\circ}\text{C}$ for 60 min, Erk was separated from other proteins by SDS-PAGE and transferred to 0.2 μm nitrocellulose membrane. The phosphorylation status of Erk was determined using an antibody to phosphorylated Erk.

Major challenges to this effort have been the dearth of small molecule lead structures that could provide starting points for the design of analogs with greater potency and selectivity, and the lack of adequate structural information to guide the synthesis of new chemical entities. The differences in the primary amino acid sequence within the catalytic domain of phosphatases such as MKP-1, MKP-3, VHR, Cdc25B, and PTP1B, suggest selective inhibitors might be achievable (Table 2). Moreover, there are significant differences in the hydropho-

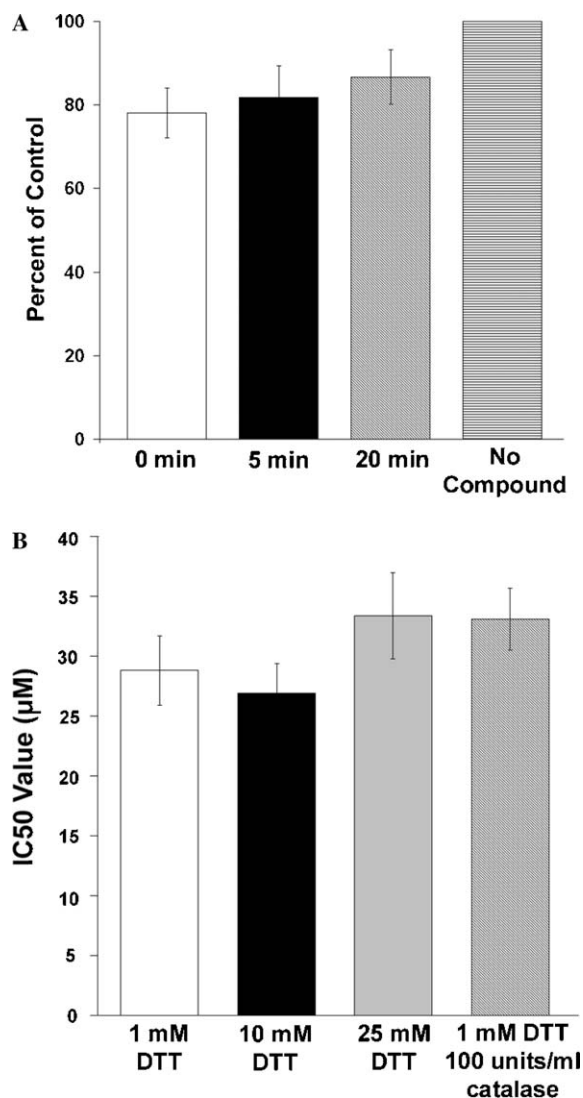


Figure 5. Reversibility of NU-126 inhibition and sensitivity to reductants and antioxidants. (A) Reversibility studies. MKP-1 was preincubated with 90 μM NU-126 or vehicle control for 0, 5 or 20 min and then diluted 20-fold with incubation buffer. The OMFP substrate was added and the remaining enzyme activity determined and compared with the vehicle control sample. (B) The IC_{50} values of NU-126 against MKP-1 in the presence of 1–25 mM DTT or 1 mM DTT and 100 U/ml catalase: the mean IC_{50} values \pm SEM ($N > 5$) are shown above the bars.

bicity, calculated α helix, and calculated beta sheet structure (Table 2). X-ray crystallographic structures for MKP-3 and PTP1B reveal architecture for the catalytic sites of these two phosphatases that are dramatically different. The dual specificity phosphatase MKP-3 displays a shallow 5.5 \AA active site cleft presumably to accommodate both the phosphotyrosine and phosphothreonine moieties. The dual specificity phosphatases VHR and Cdc25B also exhibit rather shallow active sites.^{2,22,23} In contrast, the active site cleft of the classical tyrosine phosphatase PTP1B measures 9 \AA . Structural information about MKP-1 is unavailable at this time. Nevertheless, it seems likely based on the known structural data that compounds disrupting the catalytic region will display some specificity. Moreover, positive

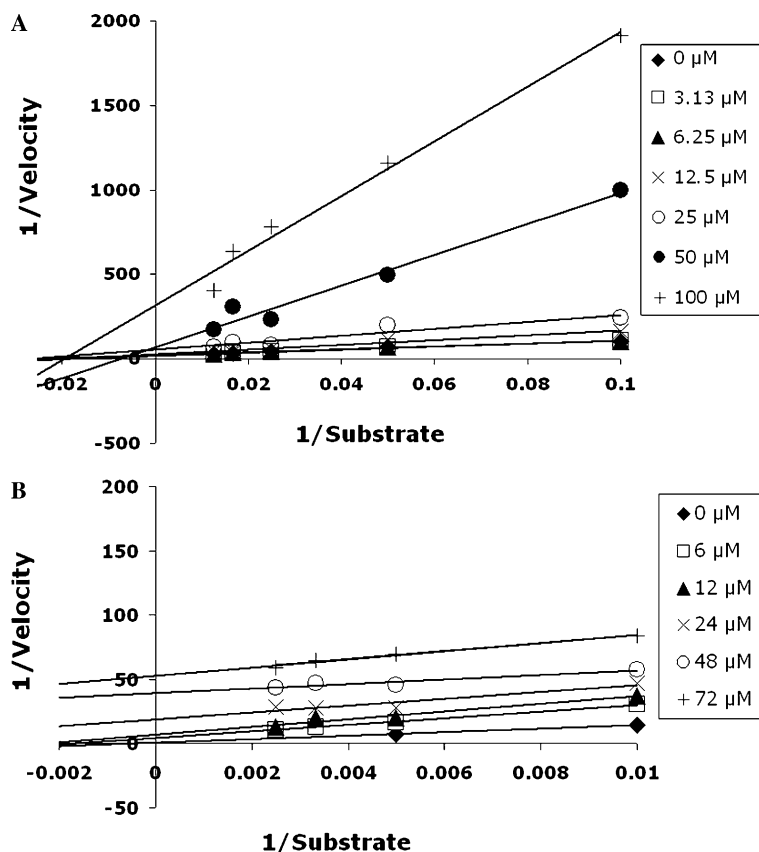


Figure 6. Kinetics of inhibition against MKP-1 and PTP1B. (A) MKP-1 was incubated with 3.2–100 μ M OMFP for 60 min at seven different concentrations of NU-126. (B) PTP1B was incubated with 3.2–100 μ M OMFP for 60 min with 6–72 μ M NU-154. Enzyme kinetics were evaluated using SigmaPlot 2000.

charges attached to the heterocyclic scaffolds appear to be beneficial for MKP-3 inhibition, but detrimental to MKP-1 binding. The results from our study with a small number of NSC 357756 analogs are consistent with this hypothesis.

It is of interest that NU-126 and NU-176 demonstrated a preference for MKP-1 compared with MKP-3, despite the 80% identity in the amino acids found in the active sites (Table 2). NU-154 had a clear preference for PTP1B compared to the other four phosphatases studied. Each of these pharmacophores provides a new platform for continued medicinal chemistry studies and the generation of novel analogs.

The catalytic activity of at least one dual specificity phosphatase, namely MKP-3, has been reported to increase six orders of magnitude after binding to its substrate Erk2; this interaction is mediated by a MAP-kinase-binding domain. It has been hypothesized that the MKP family members must undergo a conformational change upon interaction with their cognate substrate, which leads to a closure of the phosphatase activation loop.²² To ensure that the inhibition seen with the artificial small molecule substrate OMFP was indeed biochemically relevant, we examined the NU-126 inhibitory effects using both a peptide and a protein substrate. The inhibition by NU-126 was independent of the substrate. We have attempted to examine the cellular effects of NU-126 and the other ana-

logs using a previously described high content assay¹⁷ but have not detected any cellular changes. We hypothesize that these small molecules either are unable to enter cells or are rapidly degraded. Nevertheless, these novel pharmacophores should provide the foundation for the further facile refinement of small molecule inhibitors of selected protein phosphatases.

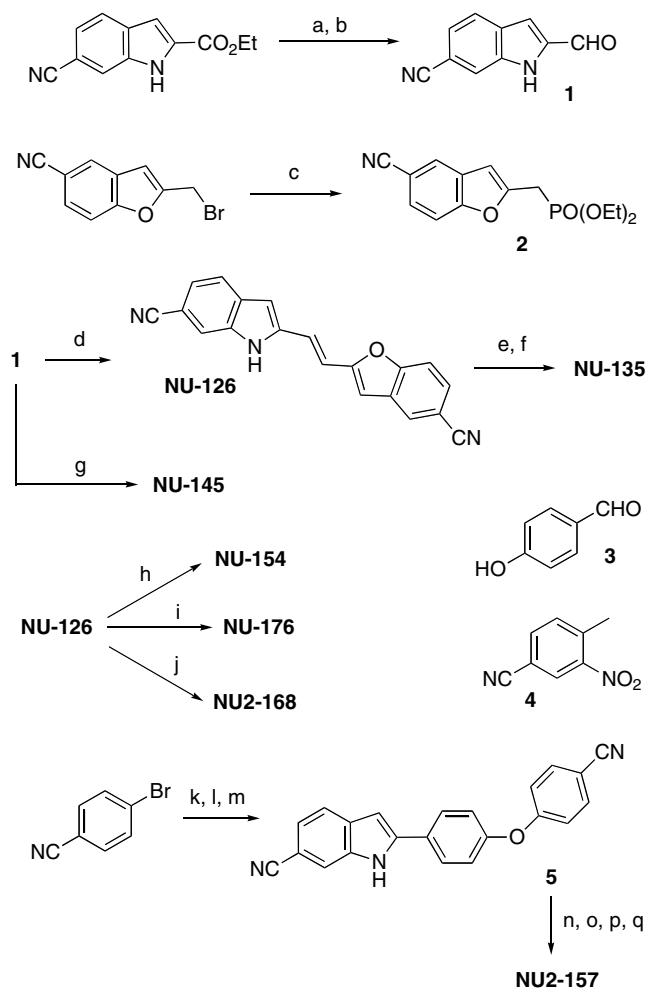
4. Materials and methods

4.1. Reagents

Epitope-tagged His₆Cdc25B₂, His₆MKP-1, and His₆MKP-3 were expressed in *Escherichia coli* and purified by Ni-NTA as previously described.²⁴ Recombinant VHR and PTP1B and the malakite green substrate were obtained from Biomol (Plymouth Meeting, PA). Unless otherwise indicated, all other reagents were obtained from Sigma-Aldrich (St. Louis, MO).

4.2. Chemical synthesis

NU-126, NU-154, NU-176, NU-2168, and NU-2157 (Fig. 1) were synthesized according to literature procedures with slight changes.^{25,26} Specifically, NU-126 was obtained by a Horner-Wittig reaction between 2-formyl-1*H*-indole-6-carbonitrile, **1**, and diethyl (5-cyanobenzofuran-2-yl)methylphosphonate, **2** (Scheme 1).



Scheme 1. Synthetic routes for new analogs. (a) LAH, THF, -78°C ; (b) MnO_2 , acetone, rt, 64% (2 steps); (c) $\text{P}(\text{OEt})_3$, xylenes, Δ , 76%; (d) **2**, MeONa , MeOH , DMF , rt, 75%; (e) Raney-Ni, $\text{NaH}_2\text{PO}_2 \cdot \text{H}_2\text{O}$, pyr/HOAc/ H_2O ; (f) aminoguanidine carbonate, THF/ EtOH , Δ , 71% (2 steps); (g) methyl diethyl phosphonoacetate, NaH , THF, rt, 58%; (h) ethylene diamine, P_2S_5 , Δ , 46%; (i) $\text{Pd}(\text{OH})_2/\text{BaSO}_4$, DMF , H_2 , rt, 66%; (j) $\text{HCl}(\text{g})$, EtOH , 0°C ; NH_3 , EtOH , rt; $\text{HCl}(\text{g})$, $\text{EtOH}/\text{Et}_2\text{O}$, rt, 58% (3 steps); (k) **3**, DMF , K_2CO_3 , 154°C , 12 h, 58%; (l) **4**, piperidine, 100°C , 6–16 h, 60%; (m) $\text{P}(\text{OEt})_3$, 160°C , 13 h, 46%; (n) $\text{HCl}(\text{g})$, EtOH , 36 h; (o) NH_3 , EtOH , 36 h; (p) HCl , Et_2O ; (q) HPLC in $\text{MeCN}/\text{H}_2\text{O}/0.1\% \text{HCO}_2\text{H}$, 60% (3 steps).

NU-126 was then condensed with ethylene diamine in the presence of catalytic amounts of phosphorus pentasulfide to afford NU-154. NU-176 was derived from catalytic hydrogenation of NU-126 with $\text{Pd}(\text{OH})_2/\text{BaSO}_4$ in DMF . Analog NU-135 was prepared by treating NU-126 with Raney-Nickel catalyst in a mixture of aqueous pyridine and acidic acid in the presence of sodium hypophosphite monohydrate, followed by the condensation of the resulting dicarboxyaldehyde with aminoguanidine carbonate in refluxing water/ethanol. Treatment of NU-126 with dry HCl gas in EtOH for 3 min at 0°C , followed by stirring at rt for 5 days, removal of the solvent, addition of EtOH saturated with ammonia gas, stirring for 18 h, evaporation of volatiles, and treatment of the residue with HCl gas in a mixture of EtOH and Et_2O resulted in NU2-168. Finally, *p*-bromobenzonitrile was condensed with **3** and **4** to give **5** after heating of the

Knoevenagel intermediate with neat triethylphosphite, and **5** was then solvolized with ethanolic HCl ; the imide was converted to the amidine with ammonia in EtOH , and the hydrochloride salt was converted to the bisformate NU2-157 upon purification by RP-HPLC (C18, isocratic conditions, H_2O (0.1% HCO_2H)/ MeCN , 70/30).

4.3. Spectroscopic data

2-Formyl-1*H*-indole-6-carbonitrile, **1**. ^1H NMR δ (300 MHz, acetone- d_6) 11.5 (br s, 1H), 10.0 (s, 1H), 7.99 (s, 1H), 7.98 (d, $J = 8.6$ Hz, 1H), 7.50 (s, 1H), 7.41 (d, $J = 8.6$ Hz, 2H).

Diethyl (5-cyanobenzofuran-2-yl)methylphosphonate, **2**. IR (KBr) 3465, 2984, 2910, 2227, 1600, 1466, 1444, 1268, 1024, 970, 814, 784 cm^{-1} ; ^1H NMR δ (300 MHz, CDCl_3) 7.59 (s, 1H), 7.26 (s, 2H), 6.52 (d, $J = 2.9$ Hz, 1H), 3.91 (q, $J = 7.0$ Hz, 4H), 3.22 (d, $J = 21.4$ Hz, 2H), 1.09 (t, $J = 7.0$ Hz, 6H); ^{13}C NMR δ (75 MHz, CDCl_3) 155.7, 151.5, 151.3, 128.7, 126.9, 124.9, 118.7, 111.4, 105.9, 104.5, 104.4, 62.1, 62.0, 27.4, 25.5, 15.7; LRMS (EI^+) 293 (M^+ , 53), 237 (26), 156 (100), 109 (80); HRMS (EI^+) calcd for $\text{C}_{14}\text{H}_{16}\text{NO}_4\text{P}$ 293.0817, found 293.0812.

(*E*)-2-(2-(5-Cyanobenzofuran-2-yl)vinyl)-1*H*-indole-6-carbonitrile, NU-126. IR (KBr) 3337 (NH), 2214 (CN), 1612, 1460, 1265 (C–O), 812 cm^{-1} ; ^1H NMR δ (300 MHz, $\text{DMSO}-d_6$) 12.1 (s, 1H), 8.15 (s, 1H), 7.83 (s, 1H), 7.78 (AB, $J = 8.5$ Hz, 1H), 7.74 (d of AB, $J = 8.5$, 1.5 Hz, 1H), 7.68 (d, $J = 8.2$, 1H), 7.37 (s, 2H), 7.31 (dd, $J = 8.2$, 1.5 Hz, 1H), 7.14 (s, 1H), 6.89 (d, $J = 0.8$ Hz, 1H); ^{13}C NMR δ (75 MHz, $\text{DMSO}-d_6$) 157.0, 156.8, 140.3, 137.0, 132.2, 130.3, 129.5, 126.9, 122.9, 122.3, 122.1, 121.2, 120.0, 117.5, 116.5, 113.1, 106.9, 106.4, 105.6, 104.4; LRMS (EI^+) 309 (M^+ , 100), 280 (9), 253 (5); HRMS (EI^+) calcd for $\text{C}_{20}\text{H}_{11}\text{N}_3\text{O}$ 309.0902, found 309.0896.

2-(((*E*)-2-(5-Methyleneaminoguanidyl)benzofuran-2-yl)vinyl)-1*H*-indole-6-methyleneaminoguanidine bis-(dihydrogencarbonate) salt, NU-135. IR (KBr) 3409, 2924, 1598, 1541 cm^{-1} ; ^1H NMR δ (300 MHz, $\text{DMSO}-d_6$) 11.4 (br s, 1H), 8.05 (s, 1H), 8.04 (s, 1H), 7.79 (s, 1H), 7.70 (d, $J = 8.4$ Hz, 1H), 7.51–7.46 (m, 4H), 7.21, 7.16 (AB, $J = 15.8$ Hz, 2H), 6.90 (s, 1H), 6.66 (s, 1H), 5.88 (br s, 4H), 5.55 (br s, 4H); ^{13}C NMR δ (75 MHz, $\text{DMSO}-d_6$) 160.4, 160.0, 155.4, 154.4, 145.4, 143.8, 137.9, 136.9, 132.6, 131.8, 129.3, 128.8, 123.6, 120.3, 118.9, 118.5, 115.0, 110.9, 109.6, 105.3, 104.9; LRMS (TOF MS ES^+) 428 ($[\text{M}+1]^+$, 100), 369 (15), 344 (13), 310 (14); HRMS (TOF MS ES^+) calcd for $\text{C}_{22}\text{H}_{22}\text{N}_9\text{O}$ 428.1923, found 428.1927.

(*E*)-Methyl 3-(6-cyano-1*H*-indol-2-yl)acrylate, NU-145. IR (KBr) 3305 (N–H), 2218 (CN), 1696 (C=O), 1641 (C–C, trans), 1287 (C–O) cm^{-1} ; ^1H NMR δ (300 MHz, acetone- d_6) 11.2 (br s, 1H), 7.82 (s, 1H), 7.76 (d, $J = 8.3$ Hz, 1H), 7.71 (d, $J = 16.1$ Hz, 1H), 7.33 (dd, $J = 8.3$, 1.2 Hz, 1H), 7.04 (d, $J = 1.2$ Hz, 1H), 6.60 (d, $J = 16.1$ Hz, 1H), 3.76 (s, 3H); ^{13}C NMR δ

(75 MHz, acetone- d_6) 167.1, 138.3, 137.7, 134.4, 132.2, 123.4, 123.0, 120.6, 119.1, 116.9, 116.1, 108.7, 106.8, 51.9; LRMS (EI^+) 226 (M^+ , 58), 194 (100), 166 (30), 140 (25); HRMS (EI^+) calcd for $\text{C}_{13}\text{H}_{10}\text{N}_2\text{O}_2$ 226.0742, found 226.0737.

2-((1*E*)-2-(5-(4,5-Dihydro-1*H*-imidazol-2-yl)benzofuran-2-yl)vinyl)-6-(1*H*-imidazol-2-yl)-1*H*-indole, NU-154. IR (KBr) 3184 (N–H), 1602 (C=C, *trans*), 1445, 1367, 1285 (C–O), 938 cm^{-1} ; ^1H NMR δ (300 MHz, DMSO- d_6) 11.7 (br s, 1H), 8.14 (s, 1H), 7.83 (s, 1H), 7.82 (d, $J = 8.6$ Hz, 1H), 7.60 (d, $J = 8.6$ Hz, 1H), 7.57–7.40 (m, 2H), 7.31, 7.28 (AB, $J = 16.3$ Hz, 2H), 7.08 (s, 1H), 6.78 (s, 1H), 3.85–3.2 (m, 10 H); ^{13}C NMR δ (75 MHz, DMSO- d_6) 164.8, 163.7, 155.4, 155.2, 138.1, 136.9, 130.3, 128.7, 125.9, 124.5, 123.3, 120.9, 120.0, 119.8, 119.0, 110.4, 105.7, 104.5, 49.5, 48.7; LRMS (EI^+) 395 (M^+ , 65), 394 (100), 353 (35), 169 (25); HRMS (EI^+) calcd for $\text{C}_{24}\text{H}_{21}\text{N}_5\text{O}$ 395.1746, found 395.1749.

2-(2-(5-Cyanobenzofuran-2-yl)ethyl)-1*H*-indole-6-carbonitrile, NU-176. Mp 239–240 °C (EtOAc/acetone/toluene); IR (KBr) 3344 (NH), 2223 (CN), 2216 (CN), 1464, 1269 (C–O), 828 cm^{-1} ; ^1H NMR δ (300 MHz, acetone- d_6) 10.7 (br s, 1H), 7.97 (s, 1H), 7.73 (s, 1H), 7.65 (AB, $J = 8.6$, 1H), 7.61 (d of AB, $J = 8.6$, 1.4, 1H), 7.60 (d, $J = 8.2$ Hz, 1H), 7.25 (dd, $J = 8.2$, 1.0 Hz, 1 H), 6.73 (s, 1H), 6.45 (s, 1H), 2.83 (s, 4H); ^{13}C NMR δ (75 MHz, DMSO- d_6) 160.6, 155.7, 143.3, 134.7, 131.5, 129.1, 127.3, 125.5, 121.6, 120.7, 120.2, 119.3, 115.3, 112.1, 105.5, 102.6, 101.4, 99.9, 27.0, 25.4; HRMS (TOF ESI^+) calcd for $\text{C}_{20}\text{H}_{13}\text{N}_3\text{ONa}$ 334.0956, found 334.0960.

(*E*)-2-(2-(5-Carbamimidoylbenzofuran-2-yl)vinyl)-1*H*-indole-6-carboximidamide bis(hydrogenchloride) salt, NU2-168. IR (KBr) 3077 (NH), 3380, 3148, 1670, 1534, 1459, 1270 cm^{-1} ; ^1H NMR δ (300 MHz, MeOD) 8.10 (s, 1H), 7.90 (s, 1H), 7.75–7.72 (m, 3H), 7.45 (AB, $J = 16.3$ Hz, 1H), 7.44 (dd, $J = 8.4$, 1.8 Hz, 1H), 7.31 (AB, $J = 16.3$ Hz, 1H), 7.06 (s, 1H), 6.89 (s, 1H); ^{13}C NMR δ (75 MHz, MeOD) 168.0, 167.6, 158.0, 157.4, 140.4, 137.3, 133.6, 130.2, 124.6, 123.6, 121.6, 121.5, 121.3, 121.1, 118.5, 116.8, 111.7, 111.4, 105.6, 104.5; HRMS (TOF ESI^+) calcd for $\text{C}_{20}\text{H}_{18}\text{N}_5\text{O}$ 344.1511, found 344.1510.

4-(4-(6-Isocyano-1*H*-indol-2-yl)phenoxy)benzonitrile, **5**. Mp 253–255 °C, (EtOH); IR (KBr) 3334 (NH), 2230, 2218, 1597, 1490, 1240, 820 cm^{-1} ; ^1H NMR δ (300 MHz, DMSO- d_6) 12.2 (s, 1H), 7.99 (d, $J = 8.2$ Hz, 2H), 7.86 (m, 3H), 7.68 (d, $J = 8.2$ Hz, 1H), 7.33 (d, $J = 8.2$ Hz, 1H), 7.26 (d, $J = 8.2$ Hz, 2H), 7.16 (d, $J = 8.2$ Hz, 2H), 7.05 (s, 1H); ^{13}C NMR δ (75 MHz, DMSO- d_6) 160.6, 154.7, 141.1, 135.9, 135.8, 134.6, 131.9, 131.8, 127.9, 127.7, 127.5, 122.2, 120.9, 120.6, 118.6, 118.4, 115.8, 105.5, 102.6, 99.5 ppm; LRMS (EI^+) 335 (M^+ , 100), 233 (15), 205 (15); HRMS (EI^+) calcd for $\text{C}_{22}\text{H}_{13}\text{N}_3\text{O}$ 335.1059, found 335.1056.

2-(4-(4-Carbamimidoylphenoxy)phenyl)-1*H*-indole-6-carboximidamide bis(hydrogenformate) salt, NU2-157. Mp 205 °C (H₂O/MeCN); IR (KBr) 3077 (NH), 2789,

1677, 1597, 1481, 1251 cm^{-1} ; ^1H NMR δ (300 MHz, MeOD) 8.52 (s, 2H), 7.96 (m, 3H), 7.85 (dt, $J = 6.9$, 2.0 Hz, 2H), 7.73 (d, $J = 8.4$ Hz, 1H) and 7.75 (dd, $J = 8.4$, 2.0 Hz, 1H); ^{13}C NMR δ (75 MHz, DMSO- d_6) 167.8, 166.9, 165.7, 165.2, 155.1, 154.9, 141.3, 136.3, 132.6, 131.6, 130.4, 128.1, 127.8, 122.9, 120.7, 120.3, 120.2, 118.7, 117.9, 111.9, 99.2; HRMS (TOF ESI^+) calcd for $\text{C}_{22}\text{H}_{20}\text{N}_5\text{O}$ 370.1668, found 370.1667.

4.4. Enzyme assays

Enzyme activities in the absence and presence of inhibitors were measured using the artificial substrate 3-*O*-methylfluorescein phosphate (OMFP) (Sigma–Aldrich, St. Louis, MO) at concentrations equal to the K_m of each enzyme and at the optimal pH for individual enzyme activity in a 96-well microtiter plate assay based on previously described methods.²⁴ The standard assay condition contained 0.02 mg/ml OMPF in an assay buffer comprising 30 mM Tris–HCl (pH 7.0), 75 mM NaCl, 1 mM EDTA, 0.33% BSA, and 1 mM DTT. Fluorescence emission from the product was measured after a 20 min (VHR and PTP1B) or 60 min (Cdc25, MKP-1, and MKP-3,) incubation period at ambient temperature with a multiwell plate reader (Cytofluor II; Applied Biosystems, Foster City, CA; excitation filter, 485 nm/20 nm bandwidth; emission filter, 530 nm/30 nm bandwidth). IC₅₀ concentrations were determined from four experiments using eight concentrations ranging from 0.78 to 400 μM and Prism 3.0 (GraphPad Software, Inc., San Diego, CA). Unbiased assignments for the best-fit model were determined using Enzyme Kinetics Module 1.0 (SPSS Inc., Chicago, IL). For the reversibility studies, we used a previously described dilution method.²¹ Briefly, the enzyme and 90 μM NU-126 or vehicle control were preincubated for 0, 5 or 20 min and then diluted 20-fold with incubation buffer. The OMFP substrate was added and the remaining enzyme activity determined and compared with the vehicle control sample. For the reductant and antioxidant studies, 1–25 mM DTT with or without 100 U/ml catalase was added during the incubation period.

In some studies the 12 amino acid phosphopeptide MAP (177–189) was used as a substrate for MKP-1 or VHR in the presence or absence of NU-126 for 30 min. Free phosphate released from the MAP (177–189) peptide was measured using a malakite green-based phosphate detection kit (Biomol Green, Plymouth Meeting, PA) as per the manufacturer's protocol. Briefly, the Biomol Green solution was added to the multiwell plate and incubated for 30 min at room temperature. Free phosphate was detected spectrophotometrically with a microtiter-plate reader at OD₆₂₀ nm. NU-126 inhibition of Erk dephosphorylation was determined by incubating recombinant His₆-tagged MKP-1 (125 ng) with tyrosine and threonine phosphorylated Erk2 (New England Biolabs; 10 ng) in final reaction mixture (15 μl) containing 30 mM Tris–HCl, pH 7.0, 75 mM NaCl, 0.67 mM EDTA, 1 mM DTT, and 0.033% bovine serum albumin. NU-126 (6.25–50 μM), sanguinarine (50 μM) or DMSO vehicle control was added and after incubation for 60 min, Erk dephosphorylation was determined by

Western blotting using 10% Tris–glycine gels and a monoclonal phospho-p44/42 MAPK antibody (Cell Signaling, catalog #91065) at 1:1000 dilution.

Acknowledgments

This work was supported in part by U.S. Public Health Service National Institutes of Health Grant CA78039 and the Fiske Drug Discovery Fund.

References and notes

- Bourdeau, A.; Dubé, N.; Tremblay, M. L. *Curr. Opin. Cell Biol.* **2005**, *17*, 203.
- Alonso, A.; Sasin, J.; Bottini, N.; Friedberg, I.; Friedberg, I.; Osterman, A.; Godzik, A.; Hunter, T.; Dixon, J.; Mustelin, T. *Cell. Signal.* **2004**, *117*, 699.
- Zhang, Z.-Y. *Acc. Chem. Res.* **2003**, *36*, 385.
- Dube, N.; Tremblay, M. L. *Biochim. Biophys. Acta* **2005**, *1754*, 108.
- Dube, N.; Bourdeau, A.; Heinonen, K. M.; Cheng, A.; Lee Loy, A.; Tremblay, M. L. *Cancer Res.* **2005**, *65*, 10088.
- Lund, I. K.; Andersen, H. S.; Iversen, L. F.; Olsen, O. H.; Moller, K. B.; Pedersen, A. K.; Ge, Y.; Holsworth, D. D.; Newman, M. J.; Axe, F. U.; Moller, N. P. *J. Biol. Chem.* **2004**, *279*, 24226.
- Alonso, A.; Rahmouni, S.; Williams, S.; van Stipdonk, M.; Jaroszewski, L.; Godzik, A.; Abraham, R. T.; Schoenberger, S. P.; Mustelin, T. *Nat. Immunol.* **2003**, *4*, 44.
- Alonso, A.; Saxena, M.; Williams, S.; Mustelin, T. *J. Biol. Chem.* **2001**, *276*, 4766.
- Todd, J. L.; Tanner, K. G.; Denu, J. M. *J. Biol. Chem.* **1999**, *274*, 13271.
- Magi-Galluzzi, C.; Mishra, R.; Fiorentino, M.; Montironi, R.; Yao, H.; Capodiceci, P.; Wishnow, K.; Kaplan, I.; Stork, P. J.; Loda, M. *Lab. Invest.* **1997**, *76*, 37.
- Liao, Q.; Guo, J.; Kleeff, J.; Zimmermann, A.; Buchler, M. W.; Korc, M.; Friess, H. *Gastroenterology* **2003**, *124*, 1830.
- Wang, H. Y.; Cheng, Z.; Malbon, C. C. *Cancer Lett.* **2003**, *191*, 229.
- Denkert, C.; Schmitt, W. D.; Berger, S.; Reles, A.; Pest, S.; Siegert, A.; Lichtenegger, W.; Dietel, M.; Hauptmann, S. *Int. J. Cancer* **2002**, *102*, 507.
- Sanchez-Perez, M.-G. M.; Williams, D.; Keyse, S. M.; Perona, R. *Oncogene* **2000**, *19*, 5142.
- Franklin, C. C.; Srikanth, S.; Kraft, A. S. *Proc. Natl. Acad. Sci. U.S.A.* **1998**, *95*, 3014.
- Small, G. W.; Shi, Y. Y.; Edmund, N. A.; Somasundaram, S.; Moore, D. T.; Orlowski, R. Z. *Mol. Pharmacol.* **2004**, *66*, 1478.
- Vogt, A.; Tamewitz, A.; Skoko, J.; Sikorski, R. P.; Giuliano, K. A.; Lazo, J. S. *J. Biol. Chem.* **2005**, *280*, 19078.
- Colombo, M. L.; Bosio, E. *Pharmacol. Rev.* **1996**, *33*, 127.
- Vogt, A.; Cooley, K. A.; Tarpley, M. G.; Wipf, P.; Lazo, J. S. *Chem. Biol.* **2003**, *10*, 1.
- Panchal, R. G.; Hermone, A. R.; Nguyen, T. L.; Wong, T. Y.; Schwarzenbacher, R.; Schmidt, J.; Lane, D.; McGrath, C.; Turk, B. E.; Burnett, J.; Aman, M. J.; Little, S.; Sausville, E. A.; Zaharevitz, D. W.; Cantley, L. C.; Liddington, R. C.; Gussio, R.; Bavari, S. *Nat. Struct. Biol.* **2004**, *11*, 67.
- Brisson, M.; Nguyen, T.; Wipf, P.; Joo, B.; Day, B. W.; Skoko, J. S.; Schreiber, E. M.; Foster, C.; Bansal, P.; Lazo, J. S. *Mol. Pharmacol.* **2005**, *68*, 1810.
- Farooq, A.; Zhou, M.-M. *Cell. Signal.* **2004**, *16*, 769.
- Lyon, M. A.; Ducruet, A. P.; Wipf, P.; Lazo, J. S. *Nat. Rev. Drug Discov.* **2001**, *1*, 961.
- Lazo, J. S.; Aslan, D. C.; Souhwick, E. C.; Cooley, K. A.; Ducruet, A. P.; Joo, B.; Vogt, A.; Wipf, P. *J. Med. Chem.* **2001**, *44*, 4042.
- Dann, O.; Fick, H.; Pietzner, B.; Walkenhorst, R.; Fernbach, E.; Zeh, D. *Liebigs Ann. Chem.* **1975**, 160.
- Dann, O.; Ruff, J.; Wolff, H. P.; Griessmeier, H. *Liebigs Ann. Chem.* **1984**, 409.